Low-bias negative differential conductance controlled by electrode separation*

Xiao-Hua Yi(衣晓华), Ran Liu(刘然), Jun-Jie Bi(毕俊杰),
Yang Jiao(焦扬), Chuan-Kui Wang(王传奎), and Zong-Liang Li(李宗良)†

School of Physics and Electronics, Shandong Normal University, Jinan 250014, *China*

(Received 27 July 2016; revised manuscript received 1 September 2016; published online 25 October 2016)

The electronic transport properties of a single thiolated arylethynylene molecule with 9,10-dihydroanthracene core, denoted as TADHA, is studied by using non-equilibrium Green's function formalism combined with ab initio calculations. The numerical results show that the TADHA molecule exhibits excellent negative differential conductance (NDC) behavior at lower bias regime as probed experimentally. The NDC behavior of TADHA molecule originates from the Stark effect of the applied bias voltage, by which the highest occupied molecular orbital (HOMO) and the HOMO-1 are pulled apart and become localized. The NDC behavior of TADHA molecular system is tunable by changing the electrode distance. Shortening the electrode separation can enhance the NDC effect which is attributed to the possible increase of coupling between the two branches of TADHA molecule.

Keywords: molecular junctions, negative differential conductance, electrode distance

PACS: 85.65.+h, 73.63.–b **DOI:** 10.1088/1674-1056/25/12/128503

1. Introduction

Negative differential conductance (NDC) in a nanoscale device has attracted increasing attention[1–6] for its promising applications in electronic devices such as switch,[7–10] amplifier,[11–13] memory,[14–16] and so on. The NDC behaviors have been observed in molecular devices based on single molecules[17,18] and on self-assembled monolayers (SAMs).[19,20] Generally, the NDC effects are rather small and often in relatively high bias regime.[16,17,21,22] However, the low-bias NDC behavior is very desirable since the configuration of molecular junction may be deformed by high bias voltage, especially at room temperature as we just investigated experimentally and theoretically. However, low-bias NDC molecular device is scarcely found in experiment. Recently, Perrin *et al.* have detected a pronounced NDC effect in a single thiolated arylethynylene molecule with 9,10-dihydroanthracene core, denoted as TADHA, in very low bias regime. They found that the applied voltage pulls the energy of the two arms of the molecule apart, which causes the current to decrease and results in the NDC behavior. They also detected that the NDC feature can be tuned by the electrode distance with shorter electrode separation, resulting in larger NDC feature.[23] In order to understand the mechanism of NDC behavior of TADHA molecule, according to density functional theory and using non-equilibrium Green's function (NEGF) formalism, we investigate the electronic transport properties of TADHA molecular junction here. The effects of electrode distance on geometric structure and NDC behavior of TADHA are studied systematically. Our numerical results show that compressing the electrode distance to further bend the molecule shortens the distance between the two branches of TADHA molecule, and consequently enhances the conductivity and NDC behavior of the molecule as probed experimentally.

2. Theoretical model and computational details

The molecular junction consists of a TADHA molecule sandwiched between two gold electrodes by the two terminal S atoms anchoring on two gold tips respectively. The whole system is divided into three regions: the extended molecule (consisting of the bare molecule and several surface layers of gold atoms), and two periodic semi-infinite electrodes. A $4\times4\times3$ unit cell is used to construct the periodic electrodes (see Fig. 1). The geometric structure of the bare TADHA molecule was optimized first in the SIESTA package with a maximum force of 0.02 eV/Å (1 Å = 0.1 nm).[24,25] After constructing the molecular junction, the extended molecule was optimized again. The relative positions of the Au atoms on each side were frozen, but the distance between the two Au clusters was relaxed during the subsequent geometric optimization. When performing the stretch and compression processes, the distance (D) between the two electrodes is adjusted. For each distance, the atoms of the TADHA molecule are relaxed by performing geometric optimization, and the gold electrodes are fixed. Then the electrode distance is elongated or compressed by adjusting the fixed Au atoms a little,

*Project supported by the National Natural Science Foundation of China (Grant Nos. 11374195 and 11405098) and the Natural Science Foundation of Shandong Province, China (Grant No. ZR2013FM006).

†Corresponding author. E-mail: lizongliang@sdnu.edu.cn

© 2016 Chinese Physical Society and IOP Publishing Ltd

and the structure of TADHA molecule in the extended system that is just optimized is taken as the initial geometry in the next optimization step.[26–29] In the SIESTA computations, the core electrons are represented by Troullier–Martin type norm-conserving pseudopotentials.[30] The Perdew–Burke–Ernzerhof exchange–correlation functional[31] is used for the generalized gradient approximation.[32] To save computational effort, a single-zeta plus polarization basis set for the Au atoms and a double-zeta plus polarization basis set for the other atoms are employed.

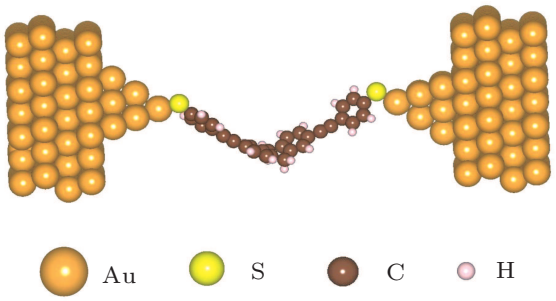


Fig. 1. (color online) Schematic structure of TADHA molecular junction.

The electronic transport properties are investigated by applying the NEGF method implemented in the TranSIESTA module of the SIESTA package. The current through the molecular junction is calculated according to the Landauer–Buttiker formula[33]

$$I = \frac{2e}{h}\int T(E,V)[f(E-\mu_{\rm L})-f(E-\mu_{\rm R})]\,{\rm d}E, \qquad (1)$$

where $T(E,V)$ is the transmission probability of incident electrons with energy E through the molecular junction under bias voltage V, $f(E)$ is the Fermi–Dirac function of the electrodes, $\mu_{\rm L}$ and $\mu_{\rm R}$ are the electrochemical potentials of the left and right electrode, respectively.

3. Results and discussion

Figure 2(a) shows the ground state energies of TADHA molecular junctions with different values of electrode distance (D). Here we set the energy of the molecular system with infinite electrode distance as the reference energy. From the figure one can see that the minimum energy which corresponds to the equilibrium electrode distance occurs at $D = 2.47$ nm. When elongating the two electrodes, the ground state energy of the molecular junction first increases slowly, and then from 2.84 nm, the energy begins to quickly increase until the molecular junction is broken at about 3.05 nm, while for compressing the electrode distance from the equilibrium point, the system energy increases slowly. The insets of Fig. 2(a) show the geometric configurations of the TADHA molecular junctions with different electrode distances. According to our calculation we find that the 9, 10-dihydroanthracene core of the TADHA molecule exhibits a dihedral of about 131.2° at the equilibrium distance, which is smaller than the dihedral of bare TADHA molecule which is 143.6°. The dihedral is gradually enlarged by stretching the electrodes (see Fig. 2(b)). When the electrode distance is stretched to 2.82 nm, the dihedral is 163.2°, while further elongating the electrodes, the 9, 10-dihydroanthracene core of the TADHA molecule is quickly converted into the plane feature, i.e., the dihedral sharply increases to about 180°. Thus further elongation of the electrode distance quickly enhances the ground state energy of the TADHA molecular junction due to the strong coupling between the terminal S atoms and the gold electrodes. From Fig. 2(b) one can find that when stretching or compressing the molecular junction, the dihedral of the 9, 10-dihydroanthracene core is very easy to adjust since it needs no more than 0.5 nN to move the two electrodes. Specifically, when the dihedral is less than 140°, the maximum force to stretch or compress TADHA molecular junction is only about 0.1 nN. However, after the 9, 10-dihydroanthracene core is flattened by stretching electrodes, the force needed to further stretch the molecular junction is sharply increased to more than 1.0 nN. Figure 2 also shows that when the electrode distance is elongated to about 3.05 nm, the TADHA molecular junction is broken. Just before the molecular junction is broken, the stretching force rises up to a maximum value of about 1.9 nN, which is obviously larger than the broken force of weak coupling systems, such as alkane diamine molecular system whose broken force is only about 0.7 nN.[29,34]

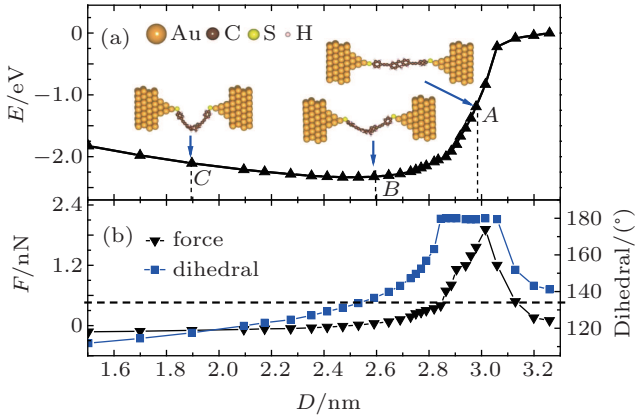


Fig. 2. (color online) Elongating and Compressing process of TADHA molecular junctions. (a) Ground state energies of TADHA molecular junctions with different values of electrode separation (D). The insets correspond to the configurations of three different distances, where B corresponds to the distance with the minimum energy, (b) Electrode force and dihedral angle of 9, 10-dihydroanthracene core versus electrode distance.

The electronic transport properties with TADHA molecular junction at the equilibrium distance are then investigated. The current and the differential conductance of TADHA molecular junction each as a function of applied bias voltage are shown in Fig. 3(a). As the figure shows, the behaviors of the current and the differential conductance are approximately

symmetric with respect to the positive and negative bias. At about ±0.25 V, the current shows peak values, at which the differential conductance shows zero value. Then with the increase of the bias, the differential conductance enters into a negative regime. The peak NDC value occurs at about 0.35 V, which is a little higher than the experimental exploration,[23] but lower than the common event.[16,17,21,22] In order to understand the NDC behavior of TADHA molecular junction, we show transmission spectra in Fig. 3(b) with bias voltages $V = 0.0$, 0.25, and 0.50 V. From the figure one can see that with the increase of the bias voltage, the transmission peak at about −0.2 eV is split into two transmission peaks. One peak shifts to near Fermi level and gradually enters into the bias window, the other peak shifts to the lower energy area and apart from the bias window. Simultaneously, the heights of the two split transmission peaks are suppressed by the bias voltage. Thus the height of the peak and the width of the bias window are competitive in the contribution to the area below the transmission curve in the bias window which is proportional to the current flow based on Eq. (1). Figure 3(b) shows that when the bias is increased from 0.25 V to 0.5 V, the mean height of transmission spectra in the bias window is suppressed to about 1/4, which thus induces the current to decrease with increasing bias, thus resulting in the NDC behavior of TADHA molecular junction.

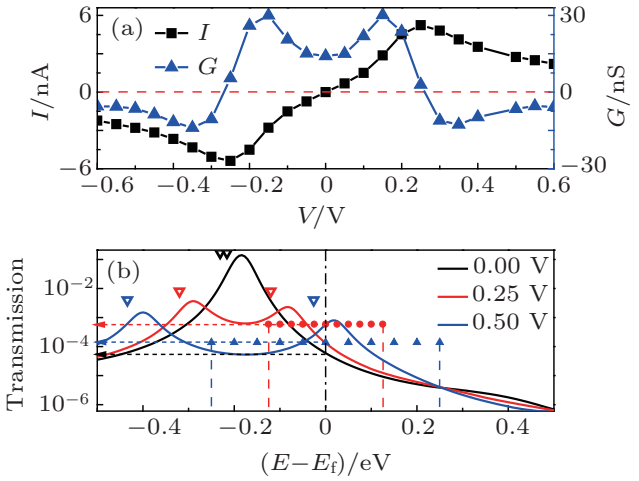


Fig. 3. (color online) Electronic transport properties of TADHA molecular junction with $D = 2.47$ nm. (a) Current and differential conductance each as a function of applied bias voltage. (b) Transmission spectra under different bias voltages.

To understand the split of the transmission peak and the NDC behavior of the TADHA molecular junction in detail, we present the molecular projected self-consistent Hamiltonian (MPSH) eigenstates which are related to these peaks in Fig. 4. The MPSH is the self-consistent Hamiltonian of the TADHA molecule with the influence of the gold electrode.[35,36] It contains the molecule–electrode coupling effects but does not contain the Hamiltonian of the gold electrode, so the MPSH eigenstates are not perfectly consistent with the eigenstates of the extended molecular system nor the positions of the transmission peaks. According to our calculations we find that these transmission peaks relate to two molecular orbitals, i.e., the highest occupied molecular orbital (HOMO) and the HOMO-1. At zero bias, these two molecular orbitals are both delocalized and almost degenerated, so they contribute a high transmission peak. When the bias voltage is applied, the degeneration of the two orbitals is destroyed due to the Stark effect of the bias. The HOMO is enhanced by the applied bias and enters into the bias window with the increase of the bias voltage, and the HOMO-1 is suppressed and apart from the bias window. Simultaneously the delocalized spatial distributions of the orbitals are also destroyed by the applied bias, with the HOMO localized on the right branch of the TADHA molecule and the HOMO-1 localized on the left branch of the TADHA molecule. It is obvious that with the separations and localizations of HOMO and HOMO-1, the single molecular orbital is a disadvantage for the electronic transport. Fortunately, the two orbitals are localized on two different branches of the TADHA molecule respectively, thus the transmission peaks related to the two orbitals can also occur due to the coupling of the two orbitals.[35,36] From Fig. 4 one can see that the spatial distributions of the HOMO and HOMO-1 present little changes, with the bias voltage enhanced from 0.25 V to 0.5 V, obviously, which is a disadvantage for the NDC effect. However, the gap between the HOMO and HOMO-1 is widened distinctly with the increase of the bias, which weakens the coupling between the two orbitals and consequently suppresses the transmission spectra and transmission peaks remarkably as figure 3 shows. Thus, although the bias window is widened by applying the voltage, the area below the transmission curve in the bias window decreases with the increase of the bias from 0.25 V, thus further resulting in the NDC behavior of TADHA molecule.

The influences of electrode separations on electronic transport properties and on NDC behaviors are then investigated. Figure 5 shows the currents and the differential conductances of TADHA molecular junction with different electrode distances. As Perrin et al. probed in the experiment,[23] the conductivity and the NDC feature of the molecular system are tunable by mechanically controlling the electrode distance. Specifically, shorter electrode separation results in not only higher conductivity, but also larger NDC effect. However, when increasing the electrode separation, the NDC behavior becomes weak. When the 9, 10-dihydroanthracene core is flattened by stretching the electrodes, the NDC behavior approximately disappears. In particular, from the current curve of $D = 2.96$ nm one can see that the TADHA molecular junction exhibits a slight rectifier behavior due to the asymmetric connection of the two interfaces between the molecule and the two electrodes.

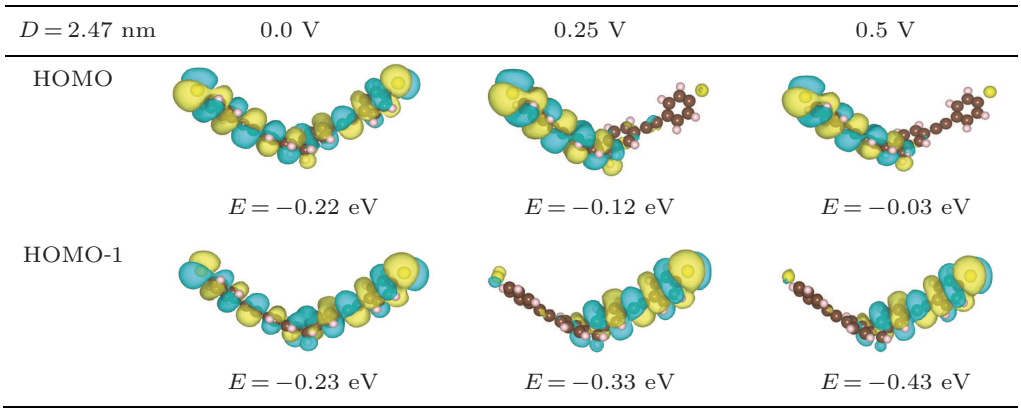


Fig. 4. (color online) Molecular orbitals contributing to the NDC behavior of TADHA molecular junction.

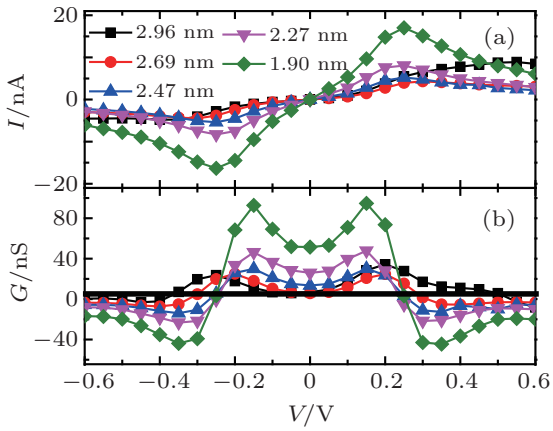


Fig. 5. (color online) (a) Currents and (b) differential conductances each as a function of bias voltage for TADHA molecular junctions with different electrode separations.

To further elucidate the distance effect on the NDC behavior of TADHA molecular junction, we show the transmission spectra in Fig. 6. Comparing Fig. 3(b) with Fig. 6(a) one can see that when shortening the electrode distance, the transmission spectra are enhanced, however, the position of the transmission peak is shifted very slightly. This is because when compressing the electrodes, the dihedral of 9, 10-dihydroanthracene core of TADHA molecule is reduced by the pressure of the electrodes, which consequently shortens the distance between the two branches of the TADHA molecule and further strengthens the coupling between the two branches which can be exhibited by the spatial distribution of MPSH eigenstates. From Fig. 7 one can clearly see that the spatial distributions of HOMO and HOMO-1 are obviously delocalized from one branch to the other branch, with the electrode distance compressed from 2.47 nm (see Fig. 4) to 1.90 nm at 0.25 V, i.e., the coupling between the two branches is strengthened by HOMO and HOMO-1, which consequently enhances the conductivity of the molecular system. On the contrary, when the 9, 10-dihydroanthracene core is flattened by stretching the electrodes, the distance between the two branches seems to be lengthened somehow, which further weakens the coupling between the two branches by the obstruction of the non-conjugated segment in the 9, 10-dihydroanthracene core, as an example one can see from Fig. 7 that the spatial distributions of the HOMO and HOMO-1 are only localized on one branch of the TADHA molecule for the electrode distance of 2.96 nm at 0.25 V, and the intervals between the eigenstates and the farther electrodes are obviously larger than those of small-electrode-distance molecular junctions. Thus in Figs. 6(b) and 6(c), the heights of the transmission peaks of $V = 0.0$ V and ± 0.25 V are suppressed and only similar to the peaks of $V = 0.50$ V, which further suppresses the NDC behavior of TADHA molecular system.

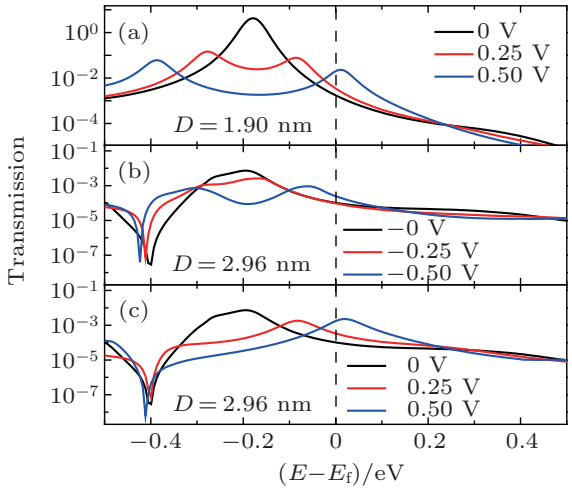


Fig. 6. (color online) Transmission spectra of TADHA molecular junction with the electrode separation $D = 1.90$ nm (a) and 2.06 nm ((b) and (c)).

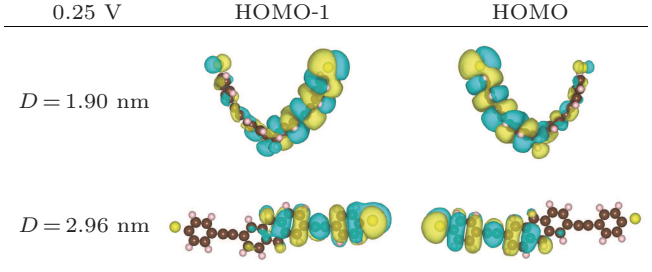


Fig. 7. (color online) Molecular orbitals at different electrode distances.

4. Conclusions

Using the density-functional theory and non-equilibrium Green's function method, the current–voltage characteristics and NDC behaviors of TADHA molecular junctions are discussed systematically. At the equilibrium electrode distance, the TADHA molecule presents a bending dihedral angle at non-conjugated segment of 9, 10-dihydroanthracene core. The TADHA molecule shows pronounced NDC behavior in lower bias regime due to the bias voltage pulling the HOMO and HOMO-1 apart. The conductivity and the NDC behavior of the molecular system can be enhanced by compressing the electrode distance, because the compressing of electrodes forces the TADHA molecule to bend more, thus strengthening the coupling between the two branches of the molecule. The elongating of the molecular junction will flatten the dihedral of the molecule and eliminate the NDC behavior of the TADHA molecular system.

References

[1] Luo W, Wang R Q, Hu L B and Yang M 2013 *Chin. Phys. B* **22** 047201
[2] Long M Q, Chen K Q, Wang L L, Zou B S and Shuai Z 2007 *Appl. Phys. Lett.* **91** 233512
[3] Zeng J, Chen K Q, He J, Zhang X J and Hu W P 2011 *Org. Electron.* **12** 1606
[4] An X T 2014 *Chin. Phys. B* **23** 107301
[5] Yu J X, Hou Z W and Liu X Y 2015 *Chin. Phys. B* **24** 067307
[6] Wu Q H, Zhao P and Liu D S 2013 *Chin. Phys. Lett.* **30** 107304
[7] Zhao P, Fang C F, Xia C J, Wang Y M, Liu D S and Xie S J 2008 *Appl. Phys. Lett.* **93** 013113
[8] An Y P, Yang Z Q and Ratner M A 2011 *J. Chem. Phys.* **135** 044706
[9] Fan Z Q, Zhang Z H, Deng X Q, Tang G P and Chen K Q 2013 *Appl. Phys. Lett.* **102** 023508
[10] Fan Z Q, Zhang Z H, Qiu M and Tang G P 2011 *Phys. Lett. A* **375** 3314
[11] Zhao J, Zeng C G, Cheng X, Wang K D, Wang G W, Yang J L, Hou J G and Zhu Q S 2005 *Phys. Rev. Lett.* **95** 045502
[12] Pan J B, Zhang Z H, Deng X Q, Qiu M and Guo C 2010 *Appl. Phys. Lett.* **97** 203104
[13] Pan J B, Zhang Z H, Deng X Q, Qiu M and Guo C 2011 *Appl. Phys. Lett.* **98** 013503
[14] You Y T, Wang M L, Xuxie H N, Wu B, Sun Z Y and Hou X Y 2010 *Appl. Phys. Lett.* **97** 233301
[15] Islam S M, Banerji P and Banerjee S 2014 *Org. Electron.* **15** 144
[16] He J and Lindsay S M 2005 *J. Am. Chem. Soc.* **127** 11932
[17] Xue Y Q, Datta S, Hong S H, Reifenberger R, Henderson J I and Kubiak C P 1999 *Phys. Rev. B* **59** 7852
[18] Gaudioso J, Lauhon L J and Ho W 2000 *Phys. Rev. Lett.* **85** 1918
[19] Kratochvilova I, Kocirik M, Zambova A, Mbindyo J, Malloukc T E and Mayer T S 2002 *J. Mater. Chem.* **12** 2927
[20] Mentovich E D, Kalifa I, Tsukernik A, Caster A, Rosenberg-Shraga N, Marom H, Gozin M and Richter S 2008 *Small* **4** 55
[21] Chen J, Reed M A, Rawlett A M and Tour J M 1999 *Science* **286** 1550
[22] Long M Q, Chen K Q, Wang L L, Wan Q, Zou B S and Shuai Z 2008 *Appl. Phys. Lett.* **92** 243303
[23] Perrin M L, Frisenda R, Koole M, Seldenthuis J S, Gil J A C, Valkenier H, Hummelen J C, Renaud N, Grozema F C, Thijssen J M, Dulić D and van der Zant H S J 2014 *Nat. Nanotech.* **9** 830
[24] Brandbyge M, Mozos J L, Ordejn P, Taylor J and Stokbro K 2002 *Phys. Rev. B* **65** 165401
[25] Soler J M, Artacho E, Gale J D, García A, Junquera J, Ordejón P and Sánchez-Portal D 2002 *J. Phys.: Condens. Matter* **14** 2745
[26] Li Z L, Zhang G P and Wang C K 2011 *J. Phys. Chem. C* **115** 15586
[27] Liu R, Bao D L, Jiao Y, Wan L W, Li Z L and Wang C K 2014 *Acta Phys. Sin.* **63** 068501 (in Chinese)
[28] Bao D L, Liu R, Leng J C, Zuo X, Jiao Y, Li Z L and Wang C K 2014 *Phys. Lett. A* **378** 1290
[29] Liu R, Wang C K and Li Z L 2016 *Sci. Rep.* **6** 21946
[30] Troullier N and Martins J L 1990 *Solid State Commun.* **74** 613
[31] Perdew J P, Burke K and Ernzerhof M 1996 *Phys. Rev. Lett.* **77** 3865
[32] Payne M C, Teter M P, Allan D C, Arias T A and Joannopoulos J D 1992 *Rev. Mod. Phys.* **64** 1045
[33] Buttiker M, Imry Y, Landauer R and Pinhas S 1985 *Phys. Rev. B* **31** 6207
[34] Frei M, Aradhya S V, Koentopp M, Hybertsen M S and Venkataraman L 2011 *Nano Lett.* **11** 1518
[35] Zhang Z H, Guo C, Kwong D J, Li J, Deng X Q and Fan Z Q 2013 *Adv. Funct. Mater.* **23** 2765
[36] Liu J, Zhu Z, Li C, Zhang Z and Qiu M 2016 *Org. Electron.* **33** 1